International Journal of Mechanical, Industrial and Aerospace Sciences
ISSN: 2517-9950
Vol:9, No:12, 2015

Singularity Loci of Actuation Schemes for 3RRR Planar Parallel Manipulator

S. Ramana Babu, V. Ramachandra Raju, K. Ramji

***Abstract*—**This paper presents the effect of actuation schemes on the performance of parallel manipulators and also how the singularity loci have been changed in the reachable workspace of the manipulator with the choice of actuation scheme to drive the manipulator. The performance of the eight possible actuation schemes of 3RRR planar parallel manipulator is compared with each other. The optimal design problem is formulated to find the manipulator geometry that maximizes the singularity free conditioned workspace for all the eight actuation cases, the optimization problem is solved by using genetic algorithms.

***Keywords*—**Actuation schemes, GCI, genetic algorithms.

I. Introduction

RECENTLY, parallel manipulators have become more popular due to their inherent advantages in terms of high stiffness, high force-to-weight ratio, high load carrying capacity, and high precision control over the prescribed path of end-effecter. However, parallel manipulator suffers from the presence of singularities within the workspace which has been explained by [1]. At singular configurations, the end-effecter will lose or gain at least one degree of freedom and the actuation forces become infinite. When the end-effecter is located close to the singularity loci the pose errors will be increased because of the influence of active joint errors; while the end-effecter approaching the singularity, the stiffness and accuracy of the manipulator deteriorates and joints may be locked up. In order to minimize the singularity loci of parallel manipulators and also to increase the performance of the manipulator, the actuation redundancy have been studied by [2]-[4]. However, in actuation redundancy, control of end-effecter is a difficult task that involves force control algorithms [5], and also requires additional expensive actuators that increase the manufacturing cost of the manipulator. Reference [6] proposed the legs of variable structure for the increase of reachable workspace of a spatial manipulator. Reference [7] studied trajectory planning and actuation schemes both are crucial for manipulator control. References [8] and [9] presented a model of an actuation scheme and its effects on the singularities of parallel manipulators for a given path in the workspace. References [10], [11] presented an efficient approach for determining the force-unconstrained poses (singularity loci) of planar parallel manipulators. The actuation scheme is the set of active input joint rates of the manipulator, one joint from each leg is to be selected. Each actuation scheme has its own singularity free zones of the end-effecter within the reachable workspace. Since each scheme implies a different set of actuator motions, this leads to different movements of the end-effecter. A proper actuation scheme not only avoids singularities of the workspace, but also enhances the stiffness and accuracy of the manipulator.

Actuation scheme of the manipulator depends on the Jacobian matrix that transforms the active input joint rates into end-effecter task space velocities. Generally, the research work on 3 dof planar parallel manipulators [12], [13] have confined to the kinematic analysis and performance of the manipulators with only one set of active joint rates (consists of only one joint from one leg) preferably the base joints. The kinematics and workspace analysis of 3dof planar parallel manipulators with other set of active joints is to be investigated. The effect of actuation schemes on the performance of 3RRR planar parallel manipulator for the positive working modes is broadly studied in this paper. Reference [14] has introduced the general aspects and working modes to allow the separation of inverse kinematic solutions; the aspects are the maximal singularity-free domains of the workspace. Based on the concept of general aspects, the performance of the actuation schemes is evaluated in limitation to positive working modes of the end-effecter.

It is well known that the singularity loci as well as the performance of the manipulator are greatly affected by the geometrical parameters of the mechanism, [15]. Many scholars have performed the optimum design of robotic manipulators; [16] proposed numerical integration and sequential quadratic programming method for optimization of parallel manipulators. However, the traditional optimization methods suffer from local optima and lack of convergence of the optimization algorithms. Reference [17] described how genetic algorithms may be applied as powerful and broadly applicable stochastic search methods and optimization techniques, since they can escape from local optima. Design of parallel manipulators while optimizing the manipulability or dexterity of the manipulator was done by [18]. Reference [19] presented an optimization approach for designing both serial and parallel manipulators.

In this work, we have also tried to enumerate the optimal geometric parameters like link lengths of a 3RRR planar parallel manipulator for each actuation scheme, which greatly influences the singularity zones of workspace and performance of the manipulator. A single objective

S. Ramana Babu is with the Raghu Engineering College, Visakhapatnam, 530022, India (phone: 91-891-2787936; fax: 91-891-2787937; e-mail: ramanababu76@ gmail.com).
V. Ramachandra Raju is with JNTUK University, Kakinada 520056, India.
K. Ramji is with the Mechanical Engineering Department, Andhra University, Visakhapatnam 530003, India.

optimization problem with GCI as the fitness function is formulated and solved using the genetic algorithm for each possible actuation scheme of 3RRR planar manipulator.

II. General description of 3RRR manipulator

The revolute joints of a planar 3-RRR parallel robot are actuated by electric DC motors because the electric actuators require minimal auxiliary support devices, which are typically a power supply and motor drive. These support devices are small and fairly portable. Secondly, the motor mass is fixed to the base frame and not part of the moving linkage mass, keeping the manipulator inertia lower. Additionally, the rotary type of actuator does not require a large base assembly and therefore the overall dimensions of the manipulator can be kept small. For these reasons the electric motor was considered the best actuator for this parallel manipulator.

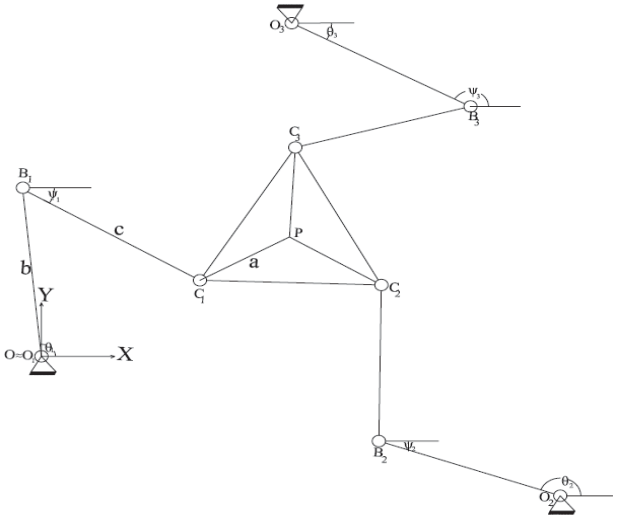

Fig. 1 3RRR parallel manipulator

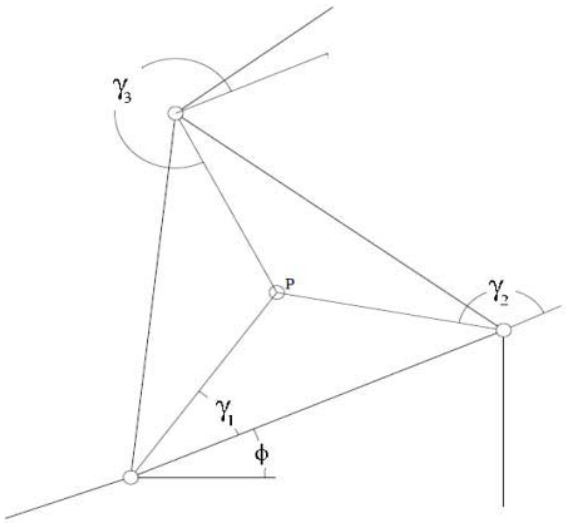

Fig. 2 End-effecter description

Figs. 1 and 2 describe the 3-RRR planar robot and its end-effecter respectively. The manipulator is actuated by three revolute actuators having only one actuator in each leg; the two links O_iB_i, B_iC_i for each leg are connected to the end-effecter by revolute joints at point C_i and to the fixed base at O_i as shown in Fig. 1. The parameters are described here without the numerical subscripts; however, when they appear with a subscript i that denotes the leg number. The geometric centre of the moving platform $C_1C_2C_3$, denoted by P is operation point (position of manipulator) in the global x-y coordinates. The end-effecter orientation $'\phi'$ is measured from the x-axis; where as b_i,c_i are length of links O_iB_i, B_iC_i respectively and a_i is the distance of point P from the revolute joint C_i.The joint angles θ_i and $\psi_i$are the orientations of links O_iB_i, B_iC_i measured from the x-axis, $\gamma_i$is the angle of the line PC_i with respect to the line connecting C_1 and C_2 on the moving platform.

A. Inverse kinematics

The vector loop closure equation for 3RRR manipulator can be expressed as:

$$\overline{\mathbf{OP}} = \overline{\mathbf{OO}_i} + \overline{\mathbf{O}_i\mathbf{B}_i} + \overline{\mathbf{B}_i\mathbf{C}_i} + \overline{\mathbf{C}_i\mathbf{P}} \tag{1}$$

Equation (1) can be expressed in the component form as

$$x_p = b\cos\theta_i + c\cos\psi_i + a\cos(\phi+\gamma_i) + x_{oi} \tag{2}$$

$$y_p = b\sin\theta_i + c\sin\psi_i + a\sin(\phi+\gamma_i) + y_{oi} \tag{3}$$

Rewriting (2) and (3) as:

$$c\cos\psi_i = x_p - b\cos\theta_i - a\cos(\phi+\gamma_i) - x_{oi} \tag{4}$$

$$c\sin\psi_i = y_p - b\sin\theta_i - a\sin(\phi+\gamma_i) - y_{oi} \tag{5}$$

Now squaring (4) and (5) then summing the two can be expressed as:

$$\begin{aligned} c^2 &= x_p^2 + y_p^2 + b^2 + a^2 + x_{oi}^2 + y_{oi}^2 - 2x_pb\cos\theta_i - 2x_pa\cos(\phi+\gamma_i) \\ &- 2x_px_{oi} + 2ab\cos\theta_i\cos(\phi+\gamma_i) + 2bx_{oi}\cos\theta_i + 2ax_{oi}\cos(\phi+\gamma_i) \\ &- 2y_pb\sin\theta_i - 2y_pa\sin(\phi+\gamma_i) - 2y_py_{oi} + 2ab\sin\theta_i\sin(\phi+\gamma_i) \\ &+ 2by_{oi}\sin\theta_i + 2ay_{oi}\sin(\phi+\gamma_i) \end{aligned} \tag{6}$$

The above equation can be expressed as:

$$e_{1i}\sin\theta_i + e_{2i}\cos\theta_i + e_{3i} = 0 \tag{7}$$

where

$$e_{1i} = -2y_pb + 2ab\sin(\phi+\gamma_i) + 2by_{oi}$$

$$e_{2i} = -2x_pb + 2ab\cos(\phi+\gamma_i) + 2bx_{oi}$$

$$e_{3i} = x_p^2 + y_p^2 + b^2 + a^2 - c^2 + x_{oi}^2 + y_{oi}^2 - 2x_pa\cos(\varphi+\gamma_i) - 2x_px_{oi}$$
$$+2ax_{oi}\cos(\varphi+\gamma_i) - 2y_pa\sin(\varphi+\gamma_i) - 2y_py_{oi} + 2ay_{oi}\sin(\varphi+\gamma_i)$$

On substitution of the trigonometric identities $\sin\theta_i = 2t_i/1+t_i^2$, $\cos\theta_i = 1-t_i^2/1+t_i^2$, in to (7) yields:

$$(e_{3i}-e_{2i})t_i^2 + 2e_{1i}t_i + (e_{3i}+e_{2i}) = 0 \tag{8}$$

where $t_i = \tan\frac{\theta_i}{2}$

Solving (8) for t_i yields:

$$\theta_i = 2\tan^{-1}\frac{-e_{1i} \pm \sqrt{e_{1i}^2 + e_{2i}^2 - e_{3i}^2}}{e_{3i}-e_{2i}} \text{ for } i = 1,2,3 \tag{9}$$

Once again rewriting (2) and (3) as

$$b\cos\theta_i = x_p - c\cos\psi_i - a\cos(\phi+\gamma_i) - x_{oi} \tag{10}$$

$$b\sin\theta_i = y_p - c\sin\psi_i - a\sin(\phi+\gamma_i) - y_{oi} \tag{11}$$

Now squaring (10) and (11) then summing the two can be expressed as

$$\begin{aligned} b^2 &= x_p^2 + y_p^2 + c^2 + a^2 + x_{oi}^2 + y_{oi}^2 - 2cx_p\cos\psi_i - 2ax_p\cos(\phi+\gamma_i) \\ &- 2x_p x_{oi} + 2ac\cos\psi_i\cos(\phi+\gamma_i) + 2cx_{oi}\cos\psi_i + 2a\cos(\phi+\gamma_i)x_{oi} \\ &- 2cy_p\sin\psi_i - 2ay_p\sin(\phi+\gamma_i) - 2y_p y_{oi} + 2ac\sin\psi_i\sin(\phi+\gamma_i) \\ &+ 2ay_{oi}\sin\psi_i + 2ay_{oi}\sin(\phi+\gamma_i) \end{aligned} \tag{12}$$

The above equation can be expressed as:

$$e_{1i}\sin\psi_i + e_{2i}\cos\psi_i + e_{3i} = 0 \tag{13}$$

where

$$e_{1i} = -2cy_p + 2ac\sin(\phi+\gamma_i) + 2cy_{oi}$$

$$e_{2i} = -2cx_p + 2ac\cos(\phi+\gamma_i) + 2cx_{oi}$$

$$\begin{aligned} e_{3i} &= x_p^2 + y_p^2 - b^2 + c^2 + a^2 + x_{oi}^2 + y_{oi}^2 - 2ax_p\cos(\phi+\gamma_i) - 2x_p x_{oi} \\ &+ 2ax_{oi}\cos(\phi+\gamma_i) - 2ay_p\sin(\phi+\gamma_i) - 2y_p y_{oi} + 2ay_{oi}\sin(\phi+\gamma_i) \end{aligned}$$

Substituting the trigonometric identities $\sin\psi_i = 2t_i/1+t_i^2$ and $\cos\psi_i = 1-t_i^2/1+t_i^2$, in to (13) yields:

$$(e_{3i}-e_{2i})t_i^2 + 2e_{1i}t_i + (e_{3i}+e_{2i}) = 0 \tag{14}$$

where $t_i = \tan\frac{\psi_i}{2}$ solving (14) for t_i yields:

$$\psi_i = 2\tan^{-1}\frac{-e_{1i} \pm \sqrt{e_{1i}^2 + e_{2i}^2 - e_{3i}^2}}{e_{3i}-e_{2i}} \quad \text{for } i = 1,2,3 \tag{15}$$

III. Actuation Schemes and Jacobian Analysis

The actuation scheme is a unique set of active joints that comprises only one joint from each leg. Since each scheme implies a different set of actuator motions, this leads to different positional movements of the end-effecter. A proper actuation scheme may ensure singularity free regions but also enhances the stiffness and accuracy of the manipulator. The actuation scheme for the mechanism depends on its actuated joints, for instance the first actuation scheme for this 3RRR mechanism is expressed as 3RRR (RRR1-RRR2 –RRR3), in this the first revolute joints of its parallel legs are actuated. Likewise, the eighth actuation scheme is expressed as 3RRR (RRR1-RRR2-RRR3) mechanism, in which the second revolute joints of its parallel legs are actuated. The underlined joints are actuated joints and the remaining joints are passive joints in the joint configuration space. The eight distinct possible actuation schemes are given in Table I.

TABLE I
Actuation Schemes

Actno	Actuation scheme	Active joint
1	RRR1-RRR2-RRR3	$\theta_1, \theta_2, \theta_3$
2	RRR1-RRR2-RRR3	ψ_1, ψ_2, ψ_3
3	RRR1-RRR2-RRR3	$\theta_1, \theta_2, \psi_3$
4	RRR1-RRR2-RRR3	$\theta_1, \psi_2, \theta_3$
5	RRR1-RRR2-RRR3	$\psi_1, \theta_2, \theta_3$
6	RRR1-RRR2-RRR3	θ_1, ψ_2, ψ_3
7	RRR1-RRR2-RRR3	ψ_1, ψ_2, θ_3
8	RRR1-RRR2-RRR3	ψ_1, θ_2, ψ_3

A. Jacobian Formulation

The Jacobian matrix for actuation scheme1 can be obtained by differentiating (6) with respect to time yields as:

$$\mathbf{J}_{x1}\dot{\mathbf{x}} = \mathbf{J}_{q1}\dot{\mathbf{q}}_1 \tag{16}$$

where

$$\mathbf{J}_{x1} = \begin{bmatrix} c_{1x} & c_{1y} & a_{1y}c_{1x} - a_{1x}c_{1y} \\ c_{2x} & c_{2y} & a_{2y}c_{2x} - a_{2x}c_{2y} \\ c_{3x} & c_{3y} & a_{3y}c_{3x} - a_{3x}c_{3y} \end{bmatrix}$$

$$\mathbf{J}_{q1} = \begin{bmatrix} b_{1x}c_{1y} - b_{1y}c_{1x} & 0 & 0 \\ 0 & b_{2x}c_{2y} - b_{2y}c_{2x} & 0 \\ 0 & 0 & b_{3x}c_{3y} - b_{3y}c_{3x} \end{bmatrix}$$

$$\dot{\mathbf{x}} = \begin{bmatrix} \dot{x}_p & \dot{y}_p & \dot{\phi} \end{bmatrix}^T,\ \dot{\mathbf{q}}_1 = \begin{bmatrix} \dot{\theta}_1 & \dot{\theta}_2 & \dot{\theta}_3 \end{bmatrix}^T$$

The Jacobian matrix for actuation scheme2 can be obtained by differentiating (12) with respect to time yields as:

$$\mathbf{J}_{x2}\dot{\mathbf{x}} = \mathbf{J}_{q2}\dot{\mathbf{q}}_2 \tag{17}$$

where

$$\mathbf{J}_{x2} = \begin{bmatrix} b_{1x} & b_{1y} & a_{1y}b_{1x} - a_{1x}b_{1y} \\ b_{2x} & b_{2y} & a_{2y}b_{2x} - a_{2x}b_{2y} \\ b_{3x} & b_{3y} & a_{3y}b_{3x} - a_{3x}b_{3y} \end{bmatrix}$$

$$\mathbf{J}_{q2}=\begin{bmatrix} b_{1y}c_{1x}-b_{1x}c_{1y} & 0 & 0 \\ 0 & b_{2y}c_{2x}-b_{2x}c_{2y} & 0 \\ 0 & 0 & b_{3y}c_{3x}-b_{3x}c_{3y} \end{bmatrix}$$

$$\dot{\mathbf{q}}_2=\begin{bmatrix}\dot{\psi}_1 & \dot{\psi}_2 & \dot{\psi}_3\end{bmatrix}^T$$

The Jacobian matrix for other actuation schemes can be expressed as:

$$\mathbf{J}_{xi}\dot{\mathbf{x}}=\mathbf{J}_{qi}\dot{\mathbf{q}}_i \qquad \text{for } i=3,...,8 \tag{18}$$

where

$$\mathbf{J}_{x3}=\begin{bmatrix} c_{1x} & c_{1y} & a_{1y}c_{1x}-a_{1x}c_{1y} \\ c_{2x} & c_{2y} & a_{2y}c_{2x}-a_{2x}c_{2y} \\ b_{3x} & b_{3y} & b_{3x}a_{3y}-b_{3y}a_{3x} \end{bmatrix}$$

$$\mathbf{J}_{q3}=\begin{bmatrix} b_{1x}c_{1y}-b_{1y}c_{1x} & 0 & 0 \\ 0 & b_{2x}c_{2y}-b_{2y}c_{2x} & 0 \\ 0 & 0 & b_{3y}c_{3x}-b_{3x}c_{3y} \end{bmatrix}$$

$$\mathbf{J}_{x4}=\begin{bmatrix} c_{1x} & c_{1y} & a_{1y}c_{1x}-a_{1x}c_{1y} \\ b_{2x} & b_{2y} & b_{2x}a_{2y}-b_{2y}a_{2x} \\ c_{3x} & c_{3y} & a_{3y}c_{3x}-a_{3x}c_{3y} \end{bmatrix}$$

$$\mathbf{J}_{q4}=\begin{bmatrix} b_{1x}c_{1y}-b_{1y}c_{1x} & 0 & 0 \\ 0 & b_{2y}c_{2x}-b_{2x}c_{2y} & 0 \\ 0 & 0 & b_{3x}c_{3y}-b_{3y}c_{3x} \end{bmatrix}$$

$$\mathbf{J}_{x5}=\begin{bmatrix} b_{1x} & b_{1y} & a_{1y}b_{1x}-a_{1x}b_{1y} \\ c_{2x} & c_{2y} & a_{2y}c_{2x}-a_{2x}c_{2y} \\ c_{3x} & c_{3y} & a_{3y}c_{3x}-a_{3x}c_{3y} \end{bmatrix}$$

$$\mathbf{J}_{q5}=\begin{bmatrix} b_{1y}c_{1x}-b_{1x}c_{1y} & 0 & 0 \\ 0 & b_{2x}c_{2y}-b_{2y}c_{2x} & 0 \\ 0 & 0 & b_{3x}c_{3y}-b_{3y}c_{3x} \end{bmatrix}$$

$$\mathbf{J}_{x6}=\begin{bmatrix} c_{1x} & c_{1y} & a_{1y}c_{1x}-a_{1x}c_{1y} \\ b_{2x} & b_{2y} & a_{2y}b_{2x}-a_{2x}b_{2y} \\ b_{3x} & b_{3y} & a_{3y}b_{3x}-a_{3x}b_{3y} \end{bmatrix}$$

$$\mathbf{J}_{q6}=\begin{bmatrix} b_{1x}c_{1y}-b_{1y}c_{1x} & 0 & 0 \\ 0 & b_{2y}c_{2x}-b_{2x}c_{2y} & 0 \\ 0 & 0 & b_{3y}c_{3x}-b_{3x}c_{3y} \end{bmatrix}$$

$$\mathbf{J}_{x7}=\begin{bmatrix} b_{1x} & b_{1y} & a_{1y}b_{1x}-a_{1x}b_{1y} \\ b_{2x} & b_{2y} & a_{2y}b_{2x}-a_{2x}b_{2y} \\ c_{3x} & c_{3y} & a_{3y}c_{3x}-a_{3x}c_{3y} \end{bmatrix}$$

$$\mathbf{J}_{q7}=\begin{bmatrix} b_{1y}c_{1x}-b_{1x}c_{1y} & 0 & 0 \\ 0 & b_{2y}c_{2x}-b_{2x}c_{2y} & 0 \\ 0 & 0 & b_{3x}c_{3y}-b_{3y}c_{3x} \end{bmatrix}$$

$$\mathbf{J}_{x8}=\begin{bmatrix} b_{1x} & b_{1y} & a_{1y}b_{1x}-a_{1x}b_{1y} \\ c_{2x} & c_{2y} & a_{2y}c_{2x}-a_{2x}c_{2y} \\ b_{3x} & b_{3y} & a_{3y}b_{3x}-a_{3x}b_{3y} \end{bmatrix}$$

$$\mathbf{J}_{q8}=\begin{bmatrix} b_{1y}c_{1x}-b_{1x}c_{1y} & 0 & 0 \\ 0 & b_{2x}c_{2y}-b_{2y}c_{2x} & 0 \\ 0 & 0 & b_{3y}c_{3x}-b_{3x}c_{3y} \end{bmatrix}$$

$$\dot{\mathbf{q}}_3=\begin{bmatrix}\dot{\theta}_1 & \dot{\theta}_2 & \dot{\psi}_3\end{bmatrix}^T,\ \dot{\mathbf{q}}_4=\begin{bmatrix}\dot{\theta}_1 & \dot{\psi}_2 & \dot{\theta}_3\end{bmatrix}^T,\ \dot{\mathbf{q}}_5=\begin{bmatrix}\dot{\psi}_1 & \dot{\theta}_2 & \dot{\theta}_3\end{bmatrix}^T$$

$$\dot{\mathbf{q}}_6=\begin{bmatrix}\dot{\psi}_1 & \dot{\theta}_2 & \dot{\psi}_3\end{bmatrix}^T,\ \dot{\mathbf{q}}_7=\begin{bmatrix}\dot{\psi}_1 & \dot{\psi}_2 & \dot{\theta}_3\end{bmatrix}^T,$$

$$\dot{\mathbf{q}}_8=\begin{bmatrix}\dot{\psi}_1 & \dot{\theta}_2 & \dot{\psi}_3\end{bmatrix}^T$$

B. Singularities of the Manipulator

Three different types of singularities were identified for parallel manipulators based on the physical interpretation of the Jacobian matrices. The singular configurations associated with inverse kinematic matrix (J_q) are called as Type I singularity it occurs when determinant of (J_q) is zero, for 3RRR manipulator such configurations are reached whenever points O_i , B_i, C_i are aligned as shown in Fig. 3. Singularity of Type II occurs when the determinant of the direct kinematic matrix (J_x) is zero. For a 3RRR actuation such configurations are reached whenever lines $(B_1C_1),(B_2C_2),(B_3C_3)$ intersect (possibly at infinity) as shown in Fig. 4; whereas for the 3RRR actuation such configurations are reached whenever lines $(O_1C_1),(O_2C_2),(O_3C_3)$ can intersect at common point as shown in Fig. 5. Singularity of Type III occurs when both J_x and J_q are singular.

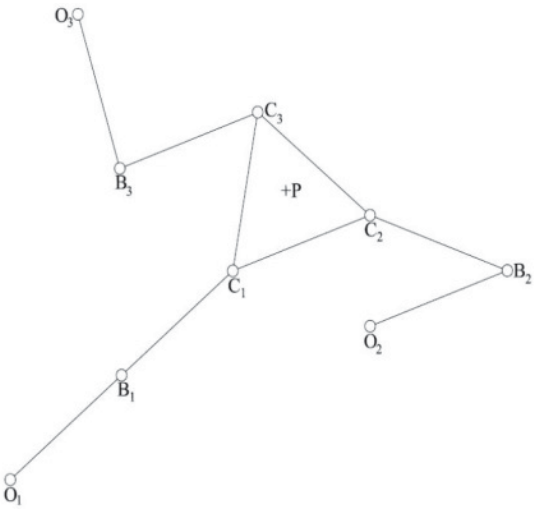

Fig. 3 Type I singularity

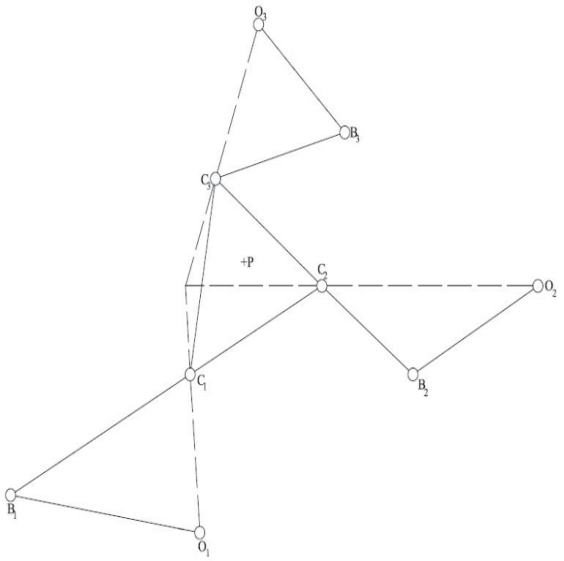

Fig. 4 Type II singularity for actuation 1

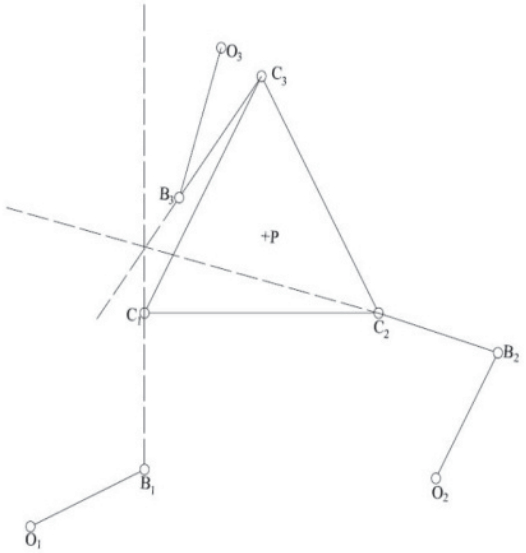

Fig. 5 Type II singularity for actuation 2

C. Global Condition Index of the Manipulator

The condition number of a Jacobian matrix is expressed as

$$k = \|\mathbf{J}\|\|\mathbf{J}^{-1}\| \tag{19}$$

Condition number signifies the error amplification factor between the joint rate errors to task space errors; the condition number depends on the manipulator configuration. The condition number varies from one at isotropic configurations to infinity at singular configurations so this is also defined as the measure of degree of ill-conditioning of the jacobian matrix. The reciprocal of the condition number ($1/\kappa$) is referred to as the conditioning index which is the local measure of performance of the manipulator at a particular pose of the end-effecter within in the workspace. In order to evaluate the global behavior of a manipulator over the workspace a global index is proposed by [20] as

$$\text{GCI} = \frac{\int_w (\frac{1}{k})dw}{\int_w dw} \tag{20}$$

where W is the workspace, κ is the condition number. In other sense, GCI is average value of reciprocal of κ over the workspace region; it represents the uniformity of dexterity over the entire workspace so this index makes sense for the optimal design of manipulator for which the average value performance is an important design factor.

IV Performance comparison of actuation schemes

The singularity loci of eight actuation schemes for the 3RRR parallel manipulator based on discretization approach are shown in Figs. 6-13. In which a continuous curve appears in green color represents the boundary of the constant workspace at $\emptyset = 0^0$, the curves which are blue in color represents the type I singularity and the curves which are in red represents the type II singularities. For all the eight actuation schemes the type I singularities are appeared as same, but the type II singularity has altered with actuation scheme. The singularity curves for actuation scheme1 (RRR1-RRR2-RRR3) shown in Fig. 6 is simple in nature and they are lied near the boundary of the workspace, whereas for the actuation scheme2 (RRR1-RRR2-RRR3) the singularities are complex in nature as shown in Fig. 7. The singularity loci for other actuations are shown in Figs. 8-13, which are altered with the actuation scheme and are passing through the different regions of the workspace.

The constant orientation workspace at $\emptyset = 0^0$ for all the eight actuation schemes are observed, from which it is observed that the maximum possible workspace is same for all the actuations which depends on geometric parameters and joint constraints. However due the presence of complex singularities the workspace is divided into some sub regions and the size of the regions under singularities over the workspace are varied from one actuation scheme to the other. The global condition index (GCI) is a measure of quality of workspace is registered different values for different actuation schemes. The performance of actuation scheme 7(R<u>R</u>R1-R<u>R</u>R2-<u>R</u>RR3) is best when compared with other actuation schemes which has attained the GCI of 0.1078, the actuation scheme 8 (R<u>R</u>R1-<u>R</u>RR2-R<u>R</u>R3) has obtained the GCI of 0.0820 it is a poor performance among all the actuations for the constant orientation workspace $\emptyset=0^0$. The actuation scheme 4 (<u>R</u>RR1-R<u>R</u>R2-<u>R</u>RR3) has attained the good performance with GCI of 0.1134 among all actuation schemes for the constant orientation workspace of $\emptyset=20^0$. From the results shown in Table II it is observed that performance is

greatly influenced by the choice of actuation for driving the mechanism.

TABLE II
PERFORMANCE OF ACTUATION SCHEMES

Actno	GCI at constant workspace of $\emptyset=0^0$	GCI for constant workspace $\emptyset=20^0$	GCI for reachable workspace
1	0.1019	0.1019	0.0982
2	0.0870	0.0817	0.0957
3	0.0897	0.0918	0.0920
4	0.1071	0.1134	0.0915
5	0.1015	0.0904	0.0840
6	0.0942	0.1022	0.0921
7	0.1078	0.0999	0.0879
8	0.0820	0.0729	0.0864

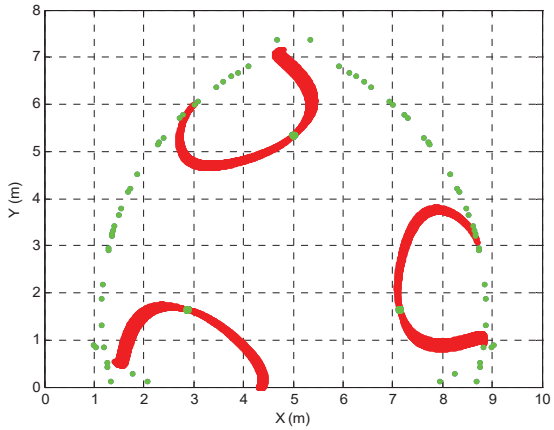

Fig. 6 Singularity loci for actuation 1

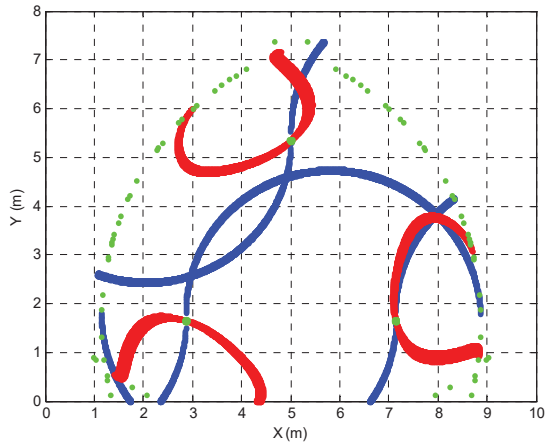

Fig. 7 Singularity loci for actuation 2

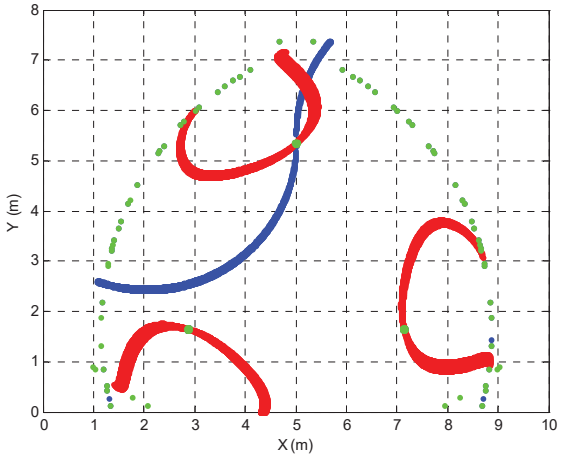

Fig. 8 Singularity loci for actuation 3

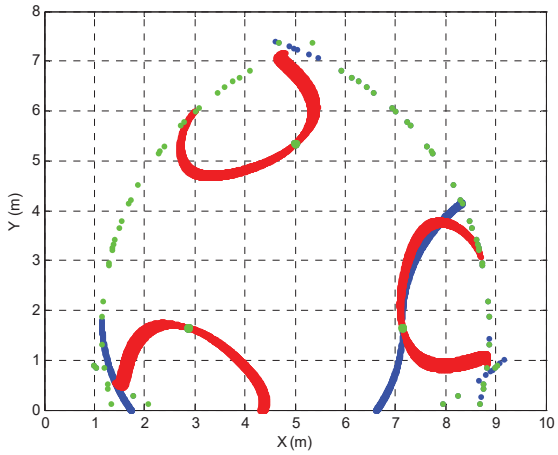

Fig. 9 Singularity loci for actuation 4

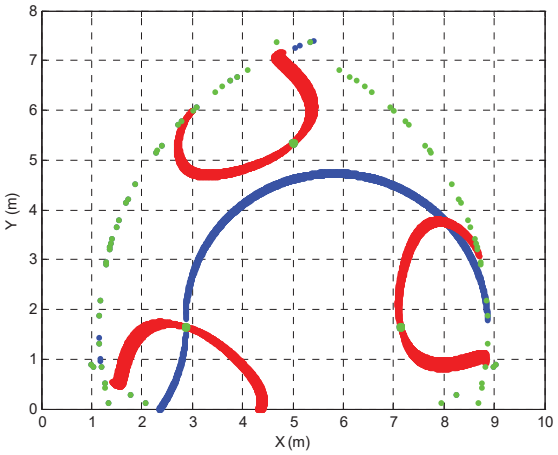

Fig. 10 Singularity loci for actuation 5

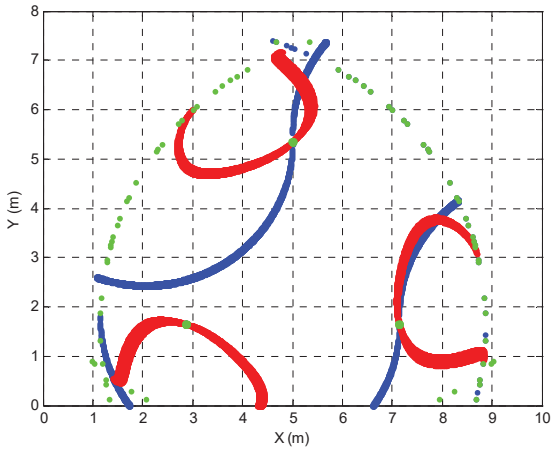

Fig. 11 Singularity loci for actuation 6

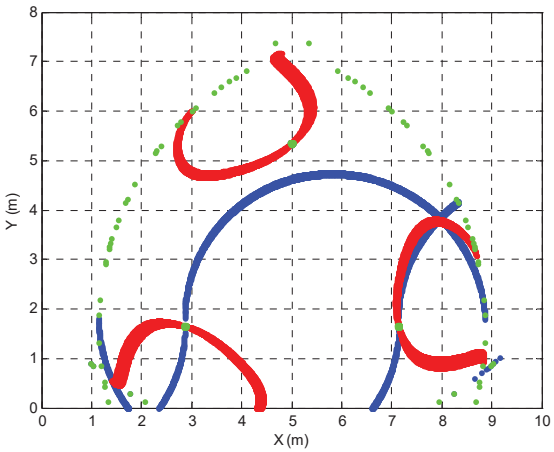

Fig. 12 Singularity loci for actuation 7

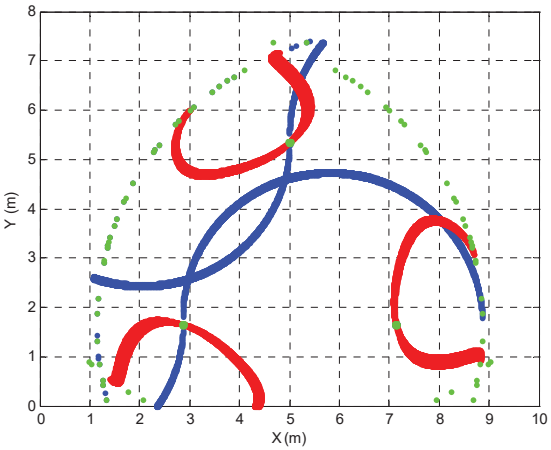

Fig. 13 Singularity loci for actuation 8

The singularity loci of all the eight actuation schemes for a constant orientation workspace at $\emptyset = 20^0$ are shown in Figs. 14-21. The Type I singularity (red in color) is same for all the actuation schemes, whereas the Type II singularities (blue in color) are varied with the actuation scheme. The Type II singularity loci for actuation scheme1 (RRR1-RRR2-RRR3) is shown in Fig. 14, which appears near the boundary of the workspace there by increasing the singularity free workspace regions for enhanced applications; whereas for the actuation scheme2 (RRR1-RRR2-RRR3) the Type II singularity loci is complex in nature which divides the workspace in to more segments as shown in Fig. 15.

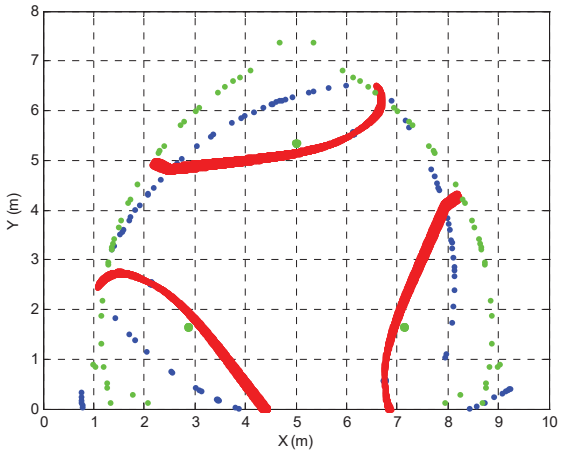

Fig. 14 Singularity loci of actuation1

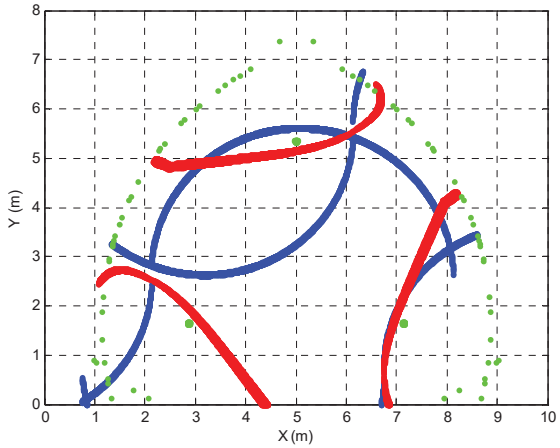

Fig. 15 Singularity loci of actuation2

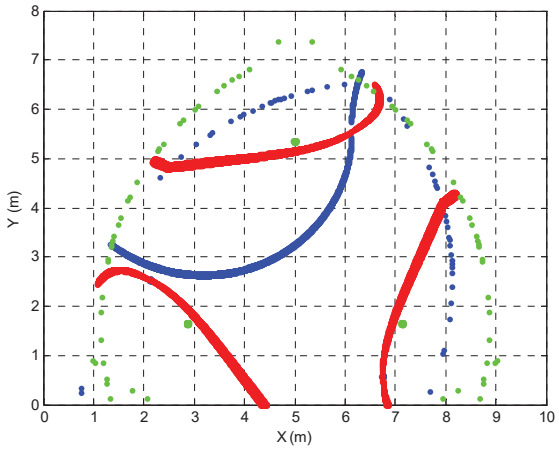

Fig. 16 Singularity loci of actuation 3

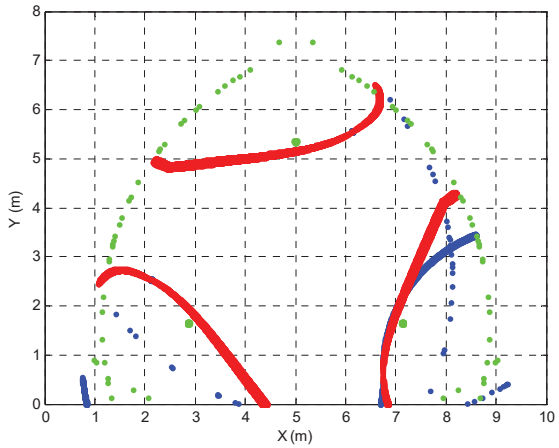

Fig. 17 Singularity loci of actuation 4

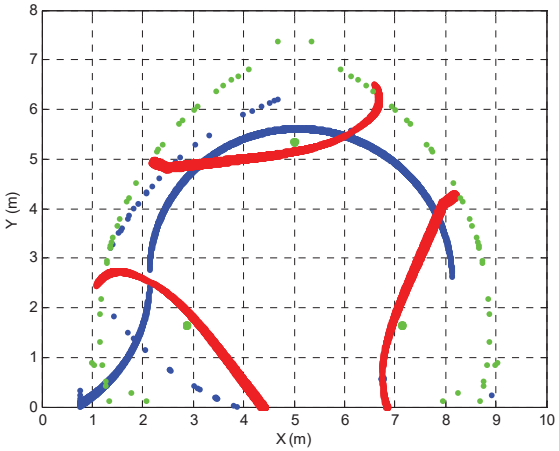

Fig. 18 Singularity loci of actuation 5

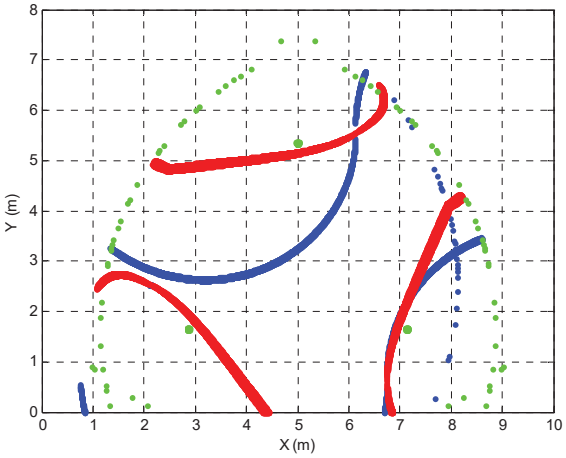

Fig. 19 Singularity loci of actuation 6

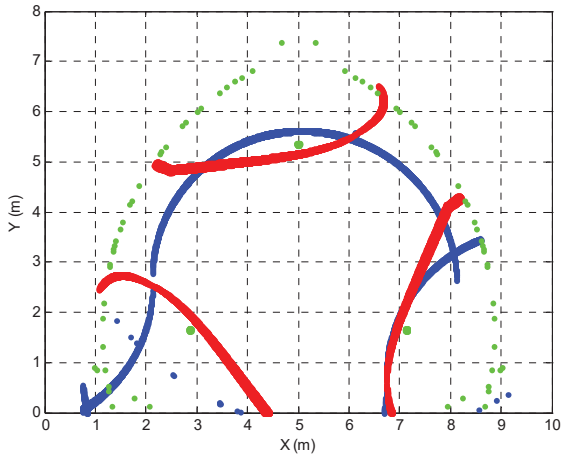

Fig. 20 Singularity loci of actuation 7

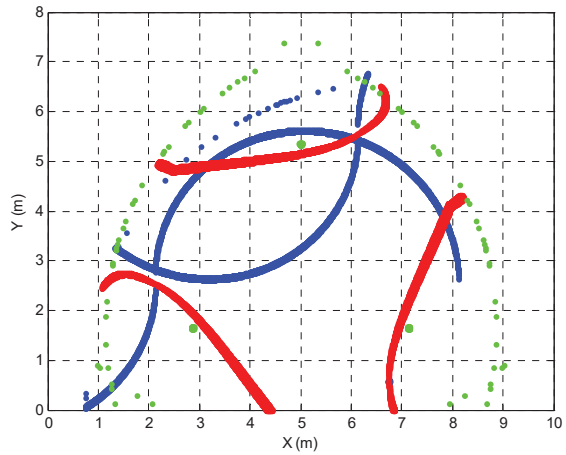

Fig. 21 Singularity loci of actuation 8

V Design Optimization

A Genetic Algorithms

GA is a meta heuristic search algorithm that uses a population of designs rather than a single design at a time and utilizes the concept of natural selection and survival of the fittest among biological structures. An initial randomized population that consists of a group of chromosomes which represent the problem variables; it produces new populations through successive iterations using various genetic operators.

B Optimal Design Problem

A single objective optimization problem for maximizing the global conditioning index as the fitness function is solved. The optimization problem is formulated as

$$\text{Max } \{GCI(x)\}$$

Subjected to $a+b+c \le \lambda$ (Constraint on manipulator size)

$$\theta_{\min i} \le \theta_i \le \theta_{\max i} \qquad i = 1,2,3$$
$$\psi_{\min i} \le \psi_i \le \psi_{\max i} \qquad i = 1,2,3 \qquad (21)$$

Ten simulation trials are performed using the MATLAB GA toolbox; the GA parameter settings are given Table III. The optimized GCI for each actuation scheme of the 3RRR parallel manipulator is given in Table IV, in which the geometric constraint $a+b+c \le 9.3$ is considered for the example problem. The GCI for all the eight actuations has greatly increased in the optimization case when compared with non optimized GCI values of actuation schemes for the randomly chosen geometric parameters. The actuation scheme1 (RRR1-RRR2-RRR3) has attained the maximum GCI of 0.3028 for the design vector of $[a \quad b \quad c]^T$=[1.300 3.251 4.000]^T among all the actuations. The optimal convergence plots for all the eight actuation schemes are shown in Figs. 22-29.

TABLE III
Simple GA Parameters

Parameter	Setting
Population size	60
Maximum generations	100
Encoding type	Real
Selection strategy	Stochastic sampling
Cross over type	Scattered
Mutation type	Adaptive

TABLE IV
Optimal Performance of Actuation Schemes

Act.no	Actuation scheme	GCI	Design vector
1	RRR1-RRR2-RRR3	0.3028	1.300 3.251 4.000
2	RRR1-RRR2-RRR3	0.2506	1.300 1.308 3.493
3	RRR1-RRR2-RRR3	0.2253	1.300 3.145 3.004
4	RRR1-RRR2-RRR3	0.2993	1.300 3.767 3.962
5	RRR1-RRR2-RRR3	0.2222	1.314 3.146 3.957
6	RRR1-RRR2-RRR3	0.2544	1.300 4.000 3.476
7	RRR1-RRR2-RRR3	0.1929	1.414 2.709 3.265
8	RRR1-RRR2-RRR3	0.1927	1.301 3.810 3.985

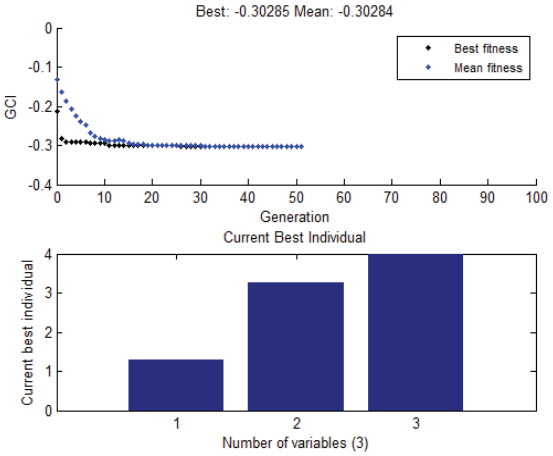

Fig. 22 Convergence of GCI for actuation 1

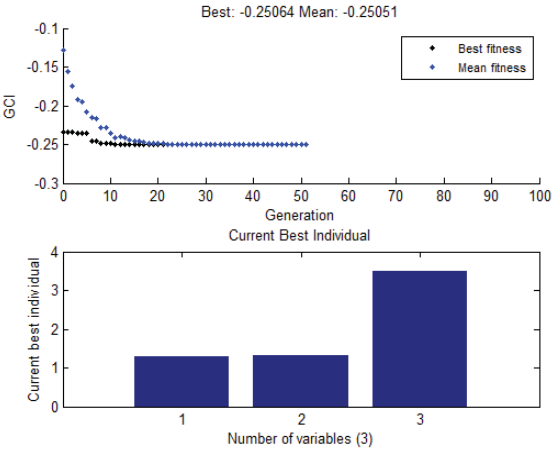

Fig. 23 Convergence of GCI for actuation 2

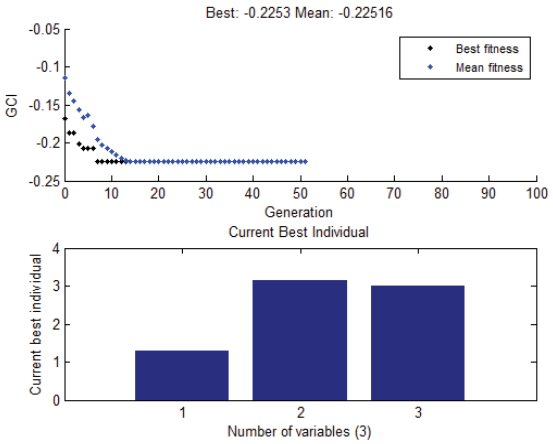

Fig. 24 Convergence of GCI for actuation 3

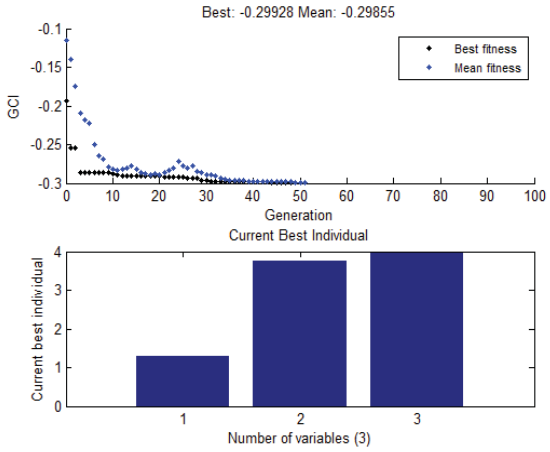

Fig. 25 Convergence of GCI for actuation 4

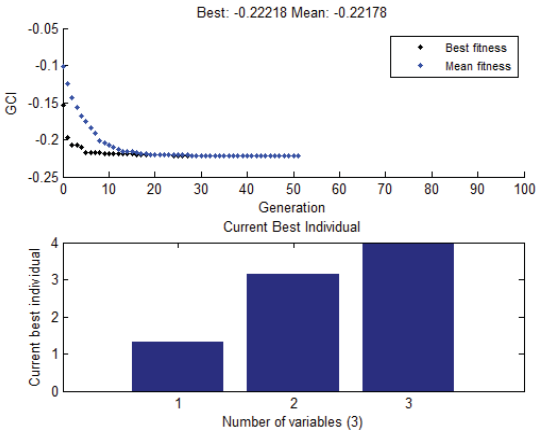

Fig. 26 Convergence of GCI for actuation 5

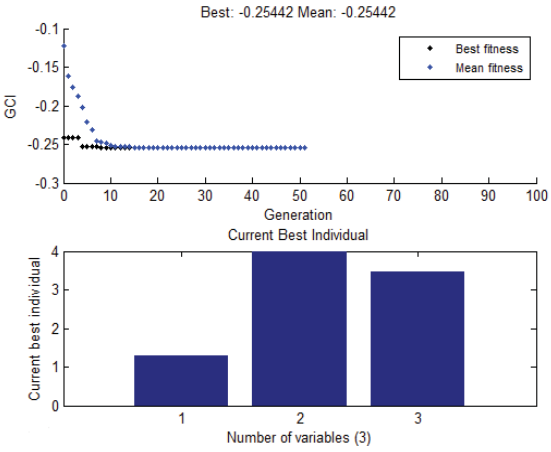

Fig. 27 Convergence of GCI for actuation 6

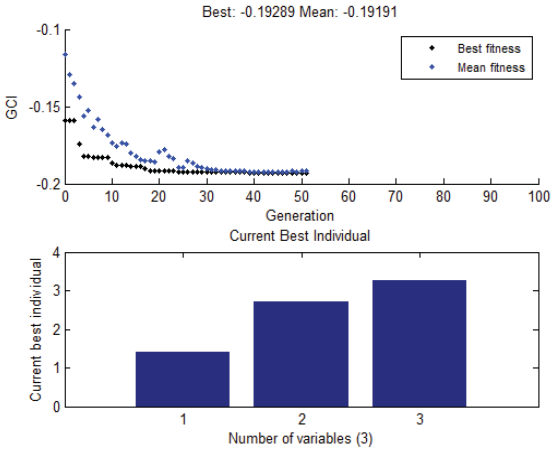

Fig. 28 Convergence of GCI for actuation 7

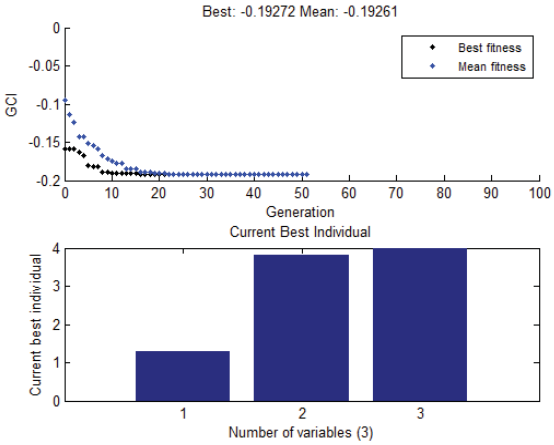

Fig. 29 Convergence of GCI for actuation 8

VI. Conclusion

The kinematic analysis of a planar 3-RRR parallel manipulator with symmetric properties is analyzed with an emphasis on actuation schemes. The kinematic singularities and reachable workspaces of all the non-redundant actuation schemes for a constant end-effecter orientation are observed. In this problem the actuation scheme is also identified as one of the design variables. It can be concluded that actuation scheme affects the performance of the manipulator (GCI) and size of the singularity free workspaces significantly. The proposed method can also be implemented for other parallel manipulators for singularity avoidance in required workspace zones.

References

[1] C. M. Gosselin and J. Angles, "Singularity analysis of closed loop kinematic chains," IEEE Transactions on Robotics and Automation, vol.6 (3), pp. 15–64, Jan. 1990.

[2] J.P. Merle, "Redundant parallel manipulators," Laboratory Robotics and Automation, vol.8 (1), pp.17-24, July 1996.

[3] S.H. Cha, T.A. Lasky and S.A. Velinsky, "Singularity avoidance for the 3RRR mechanism using kinematic Redundancy," in *Proc. 4th Annu. Allerton Conf. Robotics and Automation*, New York, 2007, pp. 1195–2000.

[4] M.G. Mohamed and C.M. Gosselin, "Design and analysis of kinematically redundant parallel manipulators with configurable platforms," IEEE Transactions on Robotics, vol.21 (3), pp.277-287, jan.2005.
[5] O. Alba-Gomez, P. Wenger and A. Pamanes, "Consistent kinetostatic indices for planar parallel manipulators: Application to the optimal kinematic inversion," in *Proc. 4th Annu. Allerton Conf. IDETC/CIE*, New York, 2005, pp. 1195–2000.
[6] V. Arakelian, S. Briot and V. Glazunov, "Increase in singularity-free zones in the workspace of parallel manipulators using mechanisms variable structure." Mechanism and Machine theory, vol.43 (9), pp.1129-1140, 2008.
[7] H.J. Su, P. Dietmaier and J.M. Macarthy, "Trajectory planning for constrained parallel manipulators," ASME Journal of Mechanical Design, vol.125 (1), pp.709-716, 2003.
[8] I. Ebrahimi, J.A. Carretero and R. Boudreau, "3PRRR redundant planar parallel manipulator: inverse displacement, workspace and singularity analyses," Mechanism and Machine theory, vol.42 (8), pp.1007-1016, 2007.
[9] N. Rakotomanga, D. Chablat and S. Caro, "Kinetostatic performance of a planar parallel mechanism with variable actuation," Advances in robot kinematics: analysis and design, vol.21, pp.311-320, 2008.
[10] F. Firamani and P. Podhorodeski, "Forced unconstrained poses for a redundantly actuated planar parallel manipulator," Mechanism and Machine Theory, vol.39, pp.459-476, 2004.
[11] F. Firmani and P. Podhorodeski, "Singularity analysis of a planar parallel manipulators based on forward kinematic solutions," Mechanism and Machine Theory, vol.44, pp.1386-1399, 2009.
[12] X-J. Liu, J.S. Wang and F. Gao, "Performance atlases of the workspace for planar 3-DOF parallel manipulators," Robotica, vol.18 (5), pp.563-568, 2000.
[13] F. Gao, X-J. Liu and X. Chen, "The relationship between the shapes of the workspace and the link lengths of 3-DOF symmetrical planar parallel manipulators, "Mechanism and Machine Theory, vol.36 (2), pp.205-220, 2001.
[14] D. Chablat and P. Wenger, "The kinematic analysis of a symmetrical three-degrees-of-freedom planar parallel manipulator, in *Conf. Rec. 2004 World Academy of Science, Engineering and Technology Int. Conf. Robot design, dynamics and control*, pp. 1–7.
[15] J. Kotlarski, B. Heimann and T. Ortmaier, "Improving the pose accuracy of a planar 3RRR parallel manipulator using kinematic redundancy and optimized switching patterns," in *Conf. Rec. 2008 IEEE Int. Conf. Robotics and Automation*, pp. 3863–3868.
[16] E.A.B. Lomonova and J.A. Andre, "Optimiation of contact less planar actuator with manipulator," IEEE T Magn, vol.44, pp.1118-1121, 2008.
[17] J. Holland, "Adaptation in natural and artificial systems, The University of Michigan press, Ann Arbor MI, 1975.
[18] G. Alici and B. Shirinadesh, "Optimum synthesis of planar parallel manipulators based on kinematic isotropy and force balancing," Robotica, vol.22, pp.97-108, 2004.
[19] M. Ceccarelli, G. Carbone and F. Ottaviano, "An optimization problem approach for designing both serial and parallel manipulators," in *Proc. MUSME International symposium multibody systems and mechatronics*, Uberlandia, 2005, pp. 6-9.
[20] C. Gosselin and J. Angeles. "A Global performance index for kinematic optimization of robotic manipulators," ASME Journal of Mechanical Design, vol.113, pp.220-226, 1991.

S. Ramana Babu was born in India in 1976. He received B.E and M.Tech degrees in mechanical engineering from Andhra University, Visakhapatnam, India, in 2001 and 2003 respectively. He is currently Assistant professor with Raghu engineering college, Visakhapatnam, India. His research interests include design optimization and motion simulation of parallel manipulators.